Optics and Lasers in Engineering 112 (2019) 16–25

Contents lists available at ScienceDirect

Optics and Lasers in Engineering

journal homepage: www.elsevier.com/locate/optlaseng

Investigation of the systematic axial measurement error caused by the space variance effect in digital holography

Yan Hao[a], Chiyue Liu[a], Jun long[a], Ping Cai[a,*], Qian Kemao[b], Anand Asundi[c]

[a] Department of Instrument Science and Engineering, School of EIEE, Shanghai Jiao Tong University, Shanghai 200240, China
[b] School of Computer Science and Engineering, Nanyang Technological University, Singapore 639798, Singapore
[c] School of Mechanical and Aerospace Engineering, Nanyang Technological University, Singapore 639798, Singapore

A B S T R A C T

Digital holography (DH) is one of the most promising quantitative phase measurement techniques and has been successfully used in 3D imaging and measurement. One of its attractive advantages is its excellent theoretical axial measurement accuracy of better than 1 nanometer. However, in practice, the axial accuracy has been quoted to be in the range of tens nanometers limited by the axial errors existing in DH system. In order to improve the axial measurement accuracy to approach the theoretical value, it is necessary to identify error sources and then reduce the errors according to their properties. In this paper, the space-variance effect of digital holography system is investigated and demonstrated to be an important systematic axial measurement error (SAME) source, especially for features with high frequency. The properties of the space-variant SAME are investigated through simulations and experiments. The object position, object height, object frequency content and object-CCD distance are found to be related to the space-variant SAME. Careful and appropriate placement of the object according to its features is thus necessary to reduce such SAME in a DH system. Based on the investigation, the guideline to appropriately position an object according to its properties is provided in this work.

1. Introduction

Digital holography (DH) [1–3] provides an easy way to obtain quantitative phase distribution containing depth information of an object and allows 3D imaging of the object. DH has thus been widely applied in microscopic 3D measurement and imaging such as 3D cell imaging [4], 3D micro-structure measurement [5], 3D micro-particles tracking [6], etc. The theoretical systematic axial measurement error (SAME) of DH is smaller than 1 nanometers, where the quantization effect of CCD pixel is considered to be the only error source [4]. However, in practice, the SAME is dramatically increased to tens of nanometers [5–9], implying the existence of other axial error sources. The phase error caused by lens aberrations has been studied [10–12], which does not happen in lensless DH. In [13], The CCD aperture size has been shown to be an important contributor to the SAME, but the error it caused is smaller than that from practical experiments [13], hinting that there exist other unrevealed error sources.

The space-variance effect (SVE) has been found to affect the lateral resolution [14,15], but its influence on the SAME remains unknown and thus examined in this paper. Lensless DH system is considered so that the phase aberrations of microscope objectives and other lenses are all excluded. Through simulation and experiments, the SAME caused by the SVE will be confirmed, from which, how to position the object being measured is discussed.

The rest of the paper is organized as follows. In Section 2, the principle of DH and the SVE are briefly introduced. In Section 3, the impact of the SVE on the SAME is examined for both point and step objects through simulation, and the results are analyzed. In Section 4, the experiments are performed to validate our analysis. In Section 5, the conclusions of this work are drawn.

2. Digital holography and its space-variance effect

In this section, the principle of off-axis DH and its SVE are briefly introduced.

2.1. Principle of DH

As shown in Fig. 1, off-axis DH includes two processes: digital recording and numerical reconstruction. In the digital recording process, a light wave illuminates the object. The object wave O is reflected by an opaque object or transmits through a transparent object, and carries the object information. The reference wave R illuminates the CCD with an angle of θ. The two waves interfere to generate the hologram $I_H(x, y)$ at the CCD plane with the following resulting intensity:

$$\begin{aligned} I_H(x, y) &= |O(x, y) + R(x, y)|^2 \\ &= |O(x, y)|^2 + |R(x, y)|^2 + R(x, y)O^*(x, y) + R^*(x, y)O(x, y) \end{aligned} \quad (1)$$

where * denotes the complex conjugate. After the sampling and digitalization by the CCD camera, a digital hologram is formed.

In the numerical reconstruction process, the third or the fourth terms of Eq. (1) can be filtered out numerically due to their spatial

* Corresponding author.
E-mail address: pcai@sjtu.edu.cn (P. Cai).

https://doi.org/10.1016/j.optlaseng.2018.06.009
Received 1 February 2018; Received in revised form 18 May 2018; Accepted 12 June 2018

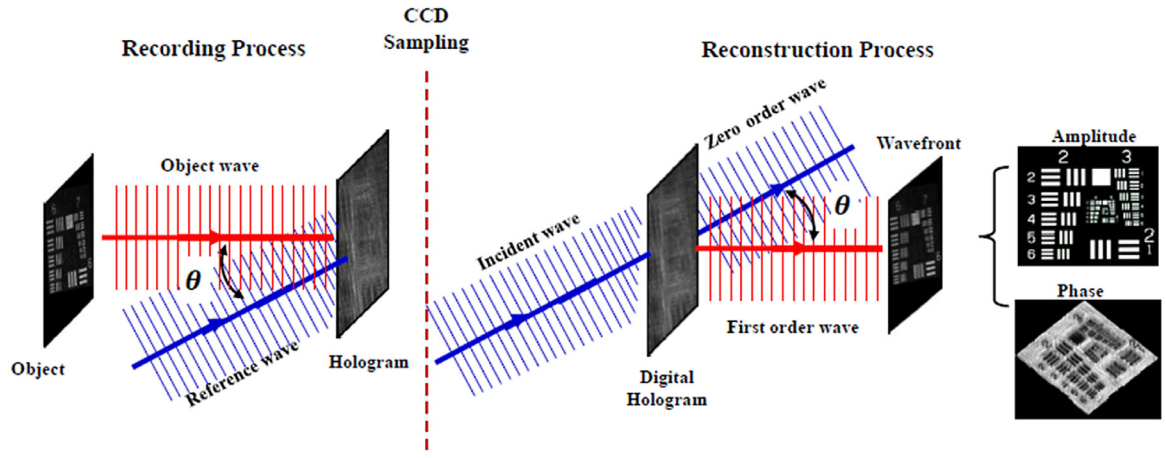

Fig. 1. An illustration of an off-axis DH system.

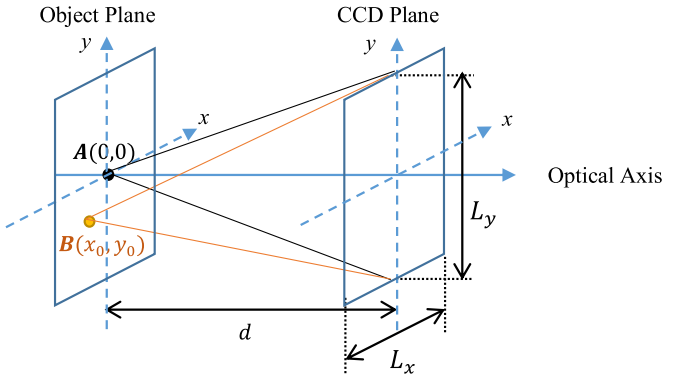

Fig. 2. An illustration of the space-variance effect of DH. The propagation and recording of the wavefronts from two points A and B.

carrier introduced by the off-axis geometry. We take the fourth term $R^*(x,y)O(x,y)$ for example. A quantitative object wavefield at the object plane can be computed from the fourth term of Eq. (1) by multiplying the reference wave $R(x,y)$ followed by Fresnel diffraction integration as [16,17]:

$$\gamma(x,y) = \mathcal{F}^{-1}\left\{\mathcal{F}\left\{R(x,y)[R^*(x,y)O(x,y)]\right\} \times G\left(f_x, f_y\right)\right\} \tag{2}$$

where $\mathcal{F}$ and $\mathcal{F}^{-1}$ denotes Fourier and inverse Fourier transforms respectively; $G(f_x, f_y)$ is the transfer function of an optical system expressed as

$$G\left(f_x, f_y\right) = \exp\left[j2\pi\frac{d}{\lambda}\sqrt{1-\left(\lambda f_x\right)^2-\left(\lambda f_y\right)^2}\right] \tag{3}$$

where λ is the laser wavelength; d is the reconstruction distance; f_x and f_y are the coordinates in the spectrum domain. The intensity and phase can be calculated as

$$I(x,y) = |\gamma(x,y)|^2, \tag{4}$$

$$\varphi(x,y) = arctan\frac{Im[\gamma(x,y)]}{Re[\gamma(x,y)]}. \tag{5}$$

From phase $\varphi(x,y)$, the desired object height in the axial direction can be obtained.

2.2. Space-variance effect of digital holography

The SVE exists in any practical systems and DH is not an exception. Two point sources A and B at different locations in Fig. 2 are used for explanation. Point A is located at $(x,y) = (0,0)$. Its propagated wavefront at the CCD plane can be written as $\exp[\frac{j\pi}{\lambda d}(x^2+y^2)]$, which will be limited by the finite CCD sensing area $L_x \times L_y$, resulting in the following truncated wavefront,

$$W_A(x,y) = \exp\left[\frac{j\pi}{\lambda d}\left(x^2+y^2\right)\right] \times \mathrm{rect}\left(\frac{x}{L_x}\right)\mathrm{rect}\left(\frac{y}{L_y}\right). \tag{6}$$

Similarly, the wavefront from point B located at $(x,y) = (x_0, y_0)$ can be written as

$$W_B(x,y) = \exp\left\{\frac{j\pi}{\lambda d}\left[\left(x-x_0\right)^2+\left(y-y_0\right)^2\right]\right\} \times \mathrm{rect}\left(\frac{x}{L_x}\right)\mathrm{rect}\left(\frac{x}{L_y}\right) \neq W_A\left(x-x_{0,}y-y_0\right), \tag{7}$$

which shows that the recording process is space-variant.

The physical process of light diffraction follows that the light containing frequency f of an object deflects from its incident direction with an angle α with a relation of $f = \frac{sin\alpha}{\lambda}$. For the point A located at $(x,y) = (0,0)$, the diffracted lights which could be collected by CCD are in the angle range of $tan\alpha \in [-\frac{L_x/2}{d}, \frac{L_x/2}{d}]$ in x direction and $tan\beta \in [-\frac{L_y/2}{d}, \frac{L_y/2}{d}]$ in y direction respectively. However, for the point B located at $(x,y) = (x_0, y_0)$, the diffracted lights collected by CCD are in the angle range of $tan\alpha \in [\frac{-L_x/2-x_0}{d}, \frac{L_x/2-x_0}{d}]$ in x direction and $tan\beta \in [\frac{-L_y/2-y_0}{d}, \frac{L_y/2-y_0}{d}]$ in y direction respectively. In practice, the distance d is usually quite large than the CCD widths L_x and L_y such that we have the approximation of $sin\alpha \cong tan\alpha$ and $sin\beta \cong tan\beta$. Hence the bandwidths of point A recorded by CCD are $(-\frac{L_x}{2\lambda d}, \frac{L_x}{2\lambda d})$ in x direction and $(-\frac{L_y}{2\lambda d}, \frac{L_y}{2\lambda d})$ in y direction while the bandwidths of point B is $(-\frac{L_x}{2\lambda d} - \frac{x_0}{\lambda d}, \frac{L_x}{2\lambda d} - \frac{x_0}{\lambda d})$ in x direction and $(-\frac{L_y}{2\lambda d} - \frac{y_0}{\lambda d}, \frac{L_y}{2\lambda d} - \frac{y_0}{\lambda d})$ in y direction respectively.

It is noticed that both bandwidths are finite but they are not the same. The finite bandwidths indicate that the CCD truncation only retains partial information of an object point. The information loss contributes to the SAME, which has been examined in [13]. The different bandwidths indicate that different points suffer different information loss and thus the ultimate SAME is also space-variant. It is thus necessary and significant to examine the severity of the non-uniformity of SAME. If this error variation is small, then the object can be freely positioned within the object plane of the DH system. Otherwise, the object positioning has to carefully follow a guideline to avoid the occurrence of severe space-variant SAME.

3. Simulation investigation of the space-variance effect on system axial measurement error

In this section, the impact of the SVE on the SAME is investigated by simulation. Simulation is adopted because the phase retrieval involving recording and reconstruction is a non-linear process and is difficult for